

Published in final edited form as:

Biochemistry. 2007 December 25; 46(51): 15123–15135. doi:10.1021/bi700736f.

Non-Nearest-Neighbor Dependence of Stability for RNA Bulge Loops Based on the Complete Set of Group I Single Nucleotide Bulge Loops†

Joshua M. Blose, Michelle L. Manni, Kelly A. Klappec, Yukiko Stranger-Jones, Allison C. Zyra, Vasiliy Sim, Chad A. Griffith, Jason D. Long, and Martin J. Serra

Department of Chemistry, Allegheny College, 520 North Main Street, Meadville PA 16335 U.S.A., Phone # 814-332-5356, Fax# 814-332-2789, Email: mserra@allegheny.edu

Fifty-nine RNA duplexes containing single nucleotide bulge loops were optically melted in 1M NaCl, and the thermodynamic parameters ΔH° , ΔS° , ΔG°_{37} , and T_M for each sequence were determined. Sequences from this study were combined with sequences from previous studies (Longfellow et al., (1990) *Biochemistry* 29, 278-285 and Znosko et al., (2002) *Biochemistry* 41, 10406-10417), thus examining all possible group I single nucleotide bulge loop and nearest-neighbor sequence combinations. The free energy increments at 37 °C for the introduction of a group I single nucleotide bulge loop ranges between 1.3 and 5.2 kcal/mol. The combined data were used to develop a model to predict the free energy of an RNA duplex containing a single nucleotide bulge. For bulge loops with adjacent Watson-Crick base pairs, neither the identity of the bulge nor the nearest-neighbor base pairs had an effect on the influence of the bulge loop on duplex stability. The proposed model for prediction of the stability of a duplex containing a bulged nucleotide was primarily affected by non-nearest-neighbor interactions. The destabilization of the duplex by the bulge was related to the stability of the stems adjacent to the bulge. Specifically, there was a direct correlation between the destabilization of the duplex and the stability of the less stable duplex stem. The stability of a duplex containing a bulged nucleotide adjacent to a wobble base pair also was primarily affected by non-nearest-neighbor interactions. Again, there was a direct correlation between the destabilization of the duplex and the stability of the less stable duplex stem. However, when one or both of the bulge nearest neighbors was a wobble base pair, the free energy increment for insertion of a bulge loop is dependent upon the position and orientation of the wobble base

pair relative the bulged nucleotide. Bulge sequences of the type $\begin{pmatrix} 5' & U & B & X \\ 3' & G & & Y \end{pmatrix}$, $\begin{pmatrix} 5' & G & B & G \\ 3' & U & & U \end{pmatrix}$, and $\begin{pmatrix} 5' & U & B & U \\ 3' & G & & G \end{pmatrix}$ are less destabilizing by 0.6 kcal/mol and bulge sequences of the type $\begin{pmatrix} 5' & G & B & X \\ 3' & U & & Y \end{pmatrix}$ and $\begin{pmatrix} 5' & X & B & U \\ 3' & Y & & G \end{pmatrix}$ are more destabilizing by 0.4 kcal/mol than bulge loops adjacent to Watson-Crick base pairs.

RNA fulfills essential cellular roles including storage of information, protein and small molecule binding, and chemical catalysis (1-10). The functional diversity of RNA is often predicated by hierarchical folding of complex tertiary structures with secondary structure formation preceding that of the native, functional fold (11,12). Since the tertiary structure arises from the preformed secondary structure, accurately determining the secondary structure of an

†This work was supported by the Camille and Henry Dreyfus Foundation, National Science Foundation Grant # MCB-0340958, and National Institutes of Health RGM-068426.

RNA molecule would provide clues to its function as well as facilitate prediction of the RNA tertiary fold. Current structure prediction algorithms using updated thermodynamic parameters correctly predict about 73% of known base pairs (13,14). Therefore, it follows that refinement of the input thermodynamic parameters for multiple secondary structure motifs would improve predictions of secondary structures. One secondary structure motif for which there remain few thermodynamic analyses is the single nucleotide bulge (15,16). A single nucleotide bulge occurs when an unpaired nucleotide disrupts regions of contiguous base pairing. These unpaired nucleotides can participate in a variety of biological events including protein binding and tertiary structure formation (17-20). More recently, single nucleotide bulges have been implicated in reverse transcriptase-mediated RNA displacement synthesis as single nucleotide bulges enhance synthesis through stable secondary structures (22).

Previously, single nucleotide bulges were subdivided into groups according to the identity of the bulge and adjacent base pairs (16). Group I single nucleotide bulge loops were defined as bulge loops where the position of the bulge was unambiguous with a bulged nucleotide that is not identical to either of the neighboring nucleotides and group II sequences were defined as bulge loops where the position of the bulge is ambiguous since the bulge nucleotide is identical to at least one of the neighboring nucleotides (Table 1). With a limited amount of data, a model was presented that provided the parameters to predict the thermodynamics of single nucleotide bulges for group I and group II bulges (16). The model for group I single nucleotide bulges, however, only examined two bulges with nearest neighbor wobble pairs. In considering the single nucleotide bulge loops with wobble base pairs, it became obvious that additional types of bulge ambiguity can arise. For example, with the oligomer 5'CGCUGCC/3'GCG CGG, the red G on the bottom strand can form a base pair with either the red C or red U. Depending upon which pair forms, either the C or the U would be the bulged nucleotide and the parent duplex would contain either a Watson-Crick or wobble base pair having different thermodynamic stabilities (Table 1). Sequences with this type of ambiguity are now defined as Group III bulge loops. Group IV single nucleotide bulge loops are defined as those sequences which have characteristics of both group II and group III sequences (Table 1). Some of the sequences originally (16) considered group I or II have now been reassigned as group III or IV.

Group I single nucleotide bulge loops are now defined as bulges with either Watson-Crick or wobble base pair nearest neighbors and no bulge ambiguity is possible. There are 26 possible Group I bulges with only Watson-Crick nearest-neighbor base pairs (Table 3) and 24 possible Group I bulges when one or more of the nearest neighbors is a wobble base pair (Table 5). Group II single nucleotide bulge loops are defined as bulges with either Watson-Crick or wobble nearest neighbors where the bulge is identical to one or more of the adjacent bases. While there is a large number of group II bulges, if more than two identical bases occur; for the case where there are only two identical bases, as in the example in Table 1, there are 68 possible sequence combinations. The possible sequence combinations are given in supporting material, Table S1. Group III single nucleotide bulge loops are defined as bulges with either an adjacent AG (GA) or CU (UC) and the possibility of forming either a Watson-Crick or wobble base pair. There are 48 possible Group III sequence combinations, they are listed in the supporting material (Table S2). There are an infinite number of Group IV single nucleotide bulge loops that have characteristics of both Group II and Group III single nucleotide bulge loops.

In the following study the complete set of group I single nucleotide bulge loops with either Watson-Crick or wobble base pair nearest neighbors has been thermodynamically characterized to improve our ability to predict the stability of RNA duplexes with bulge loops. The free energy increment for the insertion of a bulge loop into a duplex was found to be primarily influenced by non-nearest-neighbor interactions. The stability of the stem adjacent to the bulge has a direct effect on the duplex destabilization caused by the insertion of a bulge

loop. The free energy increment for group I bulges adjacent to Watson-Crick nearest neighbors is not dependent on nearest-neighbor interactions. For bulges adjacent to wobble base pair nearest neighbors, nearest-neighbor interactions influence the free energy increment for insertion of the bulge. The enthalpic contribution for insertion of a group I single nucleotide bulge loops is independent of both nearest-neighbor and non-nearest-neighbor interactions.

MATERIALS AND METHODS

RNA Synthesis and Purification

Most oligomers were synthesized on CPG solid supports (Applied Biosystems 392 DNA/RNA Synthesizer) utilizing phosphoramidites with the 2' hydroxyl protected as the *tert*-butyl dimethylsilyl ether from Glen Research (Sterling VA) (23,24). Oligomers underwent ammonia and fluoride deprotection, and crude sample was purified using preparative TLC (n-propanol:ammonium hydroxide:water, 55:35:10) and Sep-Pak C18 (Waters) chromatography. Some oligomers were ordered from Dharmacon and deprotection of the oligomers was carried out using the manufacture's instructions. The oligomers were then purified as described above. Sample purity was determined through analytical TLC or HPLC (C-8), and was greater than 95%.

Melting Curve and Data Analysis

For non-self complementary sequences, individual strand concentrations were calculated from high-temperature single strand absorbance at 260 and 280 nm using nearest-neighbor extinction coefficients (25,26). Single strands were then annealed in a 1:1 molar ratio. Optical melting experiments were performed using a Beckman DU 640 Spectrophotometer and High Performance Temperature Controller at 260 or 280 nm. Absorbance changes for oligomers in 1 M NaCl melt buffer (1 M NaCl, 0.01 M cacodylic acid, 0.5 mM EDTA, pH 7.0) were recorded as a function of temperature from 95-10°C at a rate of 1°C/min as described previously (27). The experiment was repeated at ten varying sample concentrations to give at least a 50-fold concentration range (10 µM-1mM) for each sample. Absorbance versus temperature profiles were fit to a two-state model with sloping base lines using a nonlinear least squares program (28). Thermodynamic parameters for duplex formation were obtained by two methods: (1) enthalpy and entropy changes from the fits of the individual melting curves were averaged and (2) plots of the reciprocal melting temperature, T_M^{-1} , versus $\log C_t/4$ gave enthalpy and entropy changes (29):

$$T_M^{-1} = (2.3 R / \Delta H^\circ) \log C_t / 4 + (\Delta S^\circ / \Delta H^\circ) \quad (1)$$

Here, C_t is the total concentration of oligomer. Parameters derived from the two methods generally agreed within 15%, consistent with the two-state model (30,31). The Gibbs free energy change at 37 °C was calculated as:

$$\Delta G^\circ_{37} = \Delta H^\circ - (310.15 \text{ K}) \Delta S^\circ \quad (2)$$

Determination of the contribution of bulge loops to duplex thermodynamics

The free energy of duplex formation can be approximated by the nearest-neighbor model (32). The free energy contribution of each bulged nucleotide was calculated from the experimental data and the nearest-neighbor model according to equation 3, where $\Delta G^\circ_{37(\text{measured})}$ is the experimentally determined value from the melts and

$$\Delta G^\circ_{37(\text{bulge})} = \Delta G^\circ_{37(\text{measured})} - \Delta G^\circ_{37(\text{duplex})} \quad (3)$$

$\Delta G^{\circ}_{37(\text{duplex})}$ is calculated from the nearest-neighbor model for the duplex as if it did not contain the bulge. ΔH° values are calculated in a similar fashion.

Phylogenetic Analysis

A database of phylogenetically determined RNA secondary structures (33) of 305 SSU rRNAs, 169 LSU rRNAs, 16 Group I intron RNAs and 7 Group II intron RNAs, was searched for group I single nucleotide bulge loops. The loops were characterized by nearest-neighbor base pairs and bulge identity.

Statistical Analysis

Statistical analysis of the data was done using the statistical software available with GraphPad Prism and GraphPad Instat.

RESULTS

From the study of a set of 23 oligomers containing a single nucleotide bulge loop with adjacent Watson-Crick base pairs, we have previously determined a model to predict the parameters for the thermodynamic stability of group I bulge loops (16). To more fully determine the role of the bulge identity and the nearest neighbors on the stability of bulge loops, 23 additional (12 purine and 11 pyrimidine bulges) duplexes containing a group I single nucleotide bulge loop with Watson-Crick nearest-neighbor base pairs were prepared and the thermodynamics of duplex formation measured by optical melting. These oligomers when combined with the previously measured oligomers, gives measurements for the complete set of group I single nucleotide bulge loops with by Watson-Crick nearest neighbors.

Thermodynamic parameters for duplex formation by these oligonucleotides are listed in Table 2. The oligonucleotides are listed in order of decreasing free energy for the respective duplex. Sequences were divided into two groups: duplexes with purine bulges and duplexes with pyrimidine bulges. Residues in bold are the bulge nucleotides. The parameters are the average values derived from fits of the melt curves and from T_M^{-1} versus $\log(C_t/4)$ plots. The parameters from the two methods agree within 15% for all duplexes in Table 2, suggesting that the two-state model is a reasonable approximation for these transitions (30,31). The average deviations in thermodynamic parameter values are 7.3 %, 7.9 % and 1.5 % for ΔH° , ΔS° , ΔG°_{37} , respectively.

The free energy and enthalpy contributions of each bulged nucleotide was calculated from the experimental data according to equation 3 and presented in Table 3. The complete set of all single nucleotide bulge loop duplexes used to provide the results presented in Table 3 are listed in the supporting material (Table S3) along with the thermodynamic values used to determine the values presented. As previously observed (16) all of bulges destabilize the duplex.

In our initial analysis, we focused on nearest-neighbor effects. The extent of destabilization ranges between 1.3 and 5.2 kcal/mol. Also, as noted earlier (16), on average, the pyrimidine single bulges are slightly more stable than the purine bulges by 0.3 kcal/mol. The destabilization caused by the introduction of a single group I pyrimidine bulge into a duplex is 3.9 ± 0.8 kcal/mol and for a purine bulge is 4.2 ± 0.8 kcal/mol. Since these values are not statistically different, they can be combined to provide a simple model to predict the stability of a duplex containing a single group I bulge nucleotide (purine or pyrimidine) which is just the average of all of the measured values: 4.0 ± 0.8 kcal/mol. The values in red in Table 3 represent bulge loops which appear to be less destabilizing. These values led to an understanding of the importance of non-nearest-neighbor interactions and will be discussed more fully below (see discussion).

The enthalpic increments for single nucleotide bulge loops are also presented in Tables 3. In all cases except three, the introduction of a bulge lowers the enthalpy of formation of the duplex. As with the free energy, the enthalpy contribution to duplex formation is nearly identical for pyrimidine and purine bulge nucleotides. Therefore, the enthalpy contribution for group I single nucleotide bulge loops is just the average of the measured values (13.4 ± 9.4 kcal/mol). As noted previously, the standard error for enthalpy measurements is much larger than for free energy measurements (34).

Previously, only two group I single nucleotide bulge loops adjacent to a wobble base pair had been measured (16). To determine the influence of single nucleotide bulge loops adjacent to a GU base pair, 36 additional oligonucleotide duplexes (21 purine and 15 pyrimidine bulges) were prepared and the thermodynamics of duplex formation measured by optical melting. These oligomers when combined with the previously measured oligomers, gives measurements for the complete set of group I single nucleotide bulge loops with wobble nearest-neighbor base pairs.

Thermodynamic parameters for duplex formation for oligonucleotide duplexes containing a group I single nucleotide bulge loop adjacent to a wobble base pair are listed in Table 4. The oligonucleotides are listed in order of decreasing free energy for the respective duplex. Sequences were divided into groups based upon the position and orientation of the wobble base pair relative to the position of the bulged nucleotide. Bulged nucleotides are shown in bold. The parameters are the average values derived from fits of the melt curves and from T_M^{-1} versus $\log(C_t/4)$ plots. Again, the parameters from the two methods agree within 15% for all duplexes in Table 4, suggesting that the two-state model is a reasonable approximation for these transitions. The average deviations in thermodynamic parameter values are 8.8 %, 10.3 % and 2.3 % for ΔH° , ΔS° , ΔG°_{37} , respectively.

The free energy contribution of each bulged nucleotide was calculated from the experimental data according to equation 3 and presented in Table 6. As observed for the bulges with Watson-Crick base pairs, all of bulges with wobble nearest-neighbor base pairs also destabilize the duplex. The extent of destabilization ranges between 0.5 and 5.8 kcal/mol. Given the lack of influence of the Watson-Crick nearest-neighbor base pairs to influence the thermodynamic contribution of the bulge loop to duplex formation, it seems reasonable to treat a bulge adjacent to a wobble base pair in a similar fashion.

In our initial analysis, we again focused on nearest-neighbor effects. The influence of a group I single nucleotide bulge loop adjacent to a wobble base pair depends upon both the position of the wobble pair relative to the bulge (5' or 3') and the orientation of the wobble (G or U in

the strand with the bulged nucleotide). For bulges of the type $\begin{pmatrix} 5' & G & B & X \\ 3' & U & & Y \end{pmatrix}$ and

$\begin{pmatrix} 5' & X & B & U \\ 3' & Y & & G \end{pmatrix}$ where XY is a Watson-Crick base pair, the average destabilization caused by the bulge is not significantly different than that due to bulges adjacent to Watson-Crick base

pairs, 3.2 ± 1.4 and 3.8 ± 1.7 kcal/mol, respectively. For bulges of the type $\begin{pmatrix} 5' & U & B & X \\ 3' & G & & Y \end{pmatrix}$ and bulges with two wobble nearest neighbors, the bulge is significantly less destabilizing than a bulge adjacent to Watson-Crick base pairs. The average free energy increments for

$\begin{pmatrix} 5' & U & B & X \\ 3' & G & & Y \end{pmatrix}$ and bulges with two wobble nearest neighbors, are 3.2 ± 0.7 and 2.8 ± 0.6

kcal/mol, respectively. For bulges of the type $\begin{pmatrix} 5' & X & B & G \\ 3' & Y & & U \end{pmatrix}$, the bulge is significantly more destabilizing than a bulge adjacent to Watson-Crick base pairs. The average free energy

increment is 4.5 ± 0.3 kcal/mol. The six values in red in Table 6 represent bulge loops which are less destabilizing. These values will be discussed more fully below in the context of non-nearest-neighbor interactions (see discussion).

The enthalpic increments for single nucleotide bulge loops adjacent to wobble base pairs are also presented in Tables 5. In all cases except one, the introduction of a bulge lowers the enthalpy of formation of the duplex. The enthalpy increments for insertion of a bulge loop into a duplex do not vary depending upon the position or orientation of the wobble base pair relative to the bulge. Therefore, the enthalpy contribution for group I single nucleotide bulge loops adjacent to a wobble base pair is just the average of the measured values (18.0 ± 13.6 kcal/mol).

DISCUSSION

There has been a recent explosion in nucleic acid sequence information derived from the various genome and other sequencing projects. This information provided a wealth of information about both coding and non-coding RNAs. To make full use of this information, particularly for non-coding RNAs, it is necessary to understand how the RNA sequence is related to the functionally relevant three-dimensional structure of the molecule. For this reason, there has been increased interest in predicting both the secondary and tertiary structure of RNA from sequence. The most commonly used programs for secondary structure prediction, mfold and RNAstructure (37) use thermodynamic parameters to predict the most stable (and suboptimal) secondary structural folds. The ability of these programs to predict the secondary structure depends upon the availability of accurate models to provide the thermodynamic parameters for the various RNA secondary structural motifs. Bulge loops are a common motif yet relatively few studies have investigated influence of sequence on the thermodynamics of secondary structure formation (15,16).

In an earlier investigation, using a limited number of bulge loop nucleotides, we arrived at a model to predict the parameters for the influence of bulge loops on the stability of RNA duplexes based upon the type of loop sequence (group I or II) and the identity of the bulge nucleotide when the nearest neighbors were Watson-Crick base pairs. As we began to investigate the influence of bulge loops adjacent to wobble base pairs, we came to recognize additional types of bulge loops sequences (group III and IV). In our initial investigation, some of the sequences originally identified as group I are now classified as either group III or IV. In this study, the complete set of group I single nucleotide bulge loops with either Watson-Crick or wobble base pair nearest neighbors has been thermodynamically characterized to improve our ability to predict the stability of RNA duplexes with bulge loops.

Nearest-Neighbor Influences on the Thermodynamics of Bulge Loops Adjacent to Watson-Crick Base Pairs

Since the range of thermodynamic contributions of bulge loops adjacent to Watson-Crick base pairs to duplex formation (Table 3) is relatively large, 1.3-5.4 kcal/mol, we reinvestigated the influence of the bulge nearest neighbors on the thermodynamic contribution of bulge loops on duplex formation. Figure 1 displays the plot of the free energy of the nearest-neighbor base pairs versus the free energy of the bulge. Initially, the purine and pyrimidine bulge data were plotted separately and the linear regression for each set determined. The two linear regression lines were found not to be statistically different for each other. Therefore, the two data sets were combined and the linear regression of the entire set of group I single nucleotide bulge loop data determined. The slope of the regression line (0.05 ± 0.16) was not significantly different from zero, further indicating that neither the identity of the bulge nor its nearest neighbors influence the thermodynamics for bulge loop insertion on duplex formation.

Non-Nearest-Neighbor Influences on the Thermodynamics for Bulge Loops Adjacent to Watson-Crick Base Pairs

The data highlighted in red in Table 3 were originally singled out because they seemed to represent single nucleotide bulge loops that were much less destabilizing than the remainder of the bulges examined. For example, in Table 3, the bulge sequence $\begin{pmatrix} 5' & G & C & U \\ 3' & C & & A \end{pmatrix}$, imbedded within two different duplex sequences influences the stability of the duplex by either 1.3 or 4.3 kcal/mol. In an attempt to understand the origin of the difference thermodynamic contribution of these bulges to duplex formation, we examined a number of non-nearest-neighbor factors which might contribute to the difference. The first difference we noted was that the red data points were derived from bulge loops imbedded within relatively short helix stems. Figure 2a examines the influence of helix size upon the thermodynamic contribution of the bulge to duplex formation. Although the red data points do indeed represent short helices, many of the small helices (hexamer) had bulges which were not unusually destabilizing. Next we investigated whether the stability of the parental helix was related to the thermodynamic contribution of the bulge to helix formation. This analysis is shown in Figure 2b. There was a clear relationship between the stability of the duplex and the thermodynamic contribution of the bulge to helix formation. A linear fit of the data in figure 2b gives in the following: $\Delta G^{\circ}_{37\text{bulge loop}} = (-0.27 \cdot \Delta G^{\circ}_{37\text{duplex}}) + 1.0$ ($r^2 = 0.46$). Where $\Delta G^{\circ}_{37\text{bulge loop}}$ is the free energy increment (in kcal/mol) for insertion of a bulge loop into a duplex and $\Delta G^{\circ}_{37\text{duplex}}$ is the free energy of the duplex without the bulge. Finally, we compared the stability of the less stable duplex stem with the thermodynamic contribution of the bulge to helix formation (Figure 2c). A linear fit of the data in figure 2c gives in the following: $\Delta G^{\circ}_{37\text{bulge loop}} = (-0.51 \cdot \Delta G^{\circ}_{37\text{duplex}}) + 1.0$ ($r^2 = 0.32$). The bulge loops which are less destabilizing to duplex formation (in red in Table 3) are found inserted into duplexes where the duplex or one of its stems are relatively unstable. While the fit to the data in Figure 2c is not as good as in Figure 2b, inclusion of the data for bulge loops adjacent to wobble base pairs gives a more meaningful relationship (see below).

Non-Nearest-Neighbor Influences on the Thermodynamics for Bulge Loops Adjacent to Wobble Base Pairs

A similar non-nearest-neighbor analysis of the data for bulge loops adjacent to a wobble base pair is presented in Figure 3. The data for the bulge loops adjacent to Watson-Crick base pairs is included in Figure 3 for comparison. Figure 3a examines the influence of helix length upon the thermodynamic contribution of the bulge to duplex formation. For the bulges adjacent to wobble base pairs, several of the less destabilizing bulges were found within longer duplexes of seven or eight base pairs and as seen for the bulges adjacent to Watson-Crick base pairs, many of the small helices (hexamer) had bulges which were not unusually less destabilizing. Next we investigated whether the stability of the parental helix was related to the thermodynamic contribution of the bulge to helix formation. This analysis is shown in Figure 3b. As for the bulges adjacent to Watson-Crick base pairs, there was a relationship between the stability of the duplex and the thermodynamic contribution of the bulge to helix formation. A linear fit of the data for bulge loops adjacent to wobble base pairs gives the following: $\Delta G^{\circ}_{37\text{bulge loop}} = (-0.42 \cdot \Delta G^{\circ}_{37\text{duplex}}) - 0.7$ ($r^2 = 0.37$). This line was not significantly different than the line for the bulge loops adjacent to Watson-Crick base pair, so both sets of data were combined. The linear fit for the combined data give the following: $\Delta G^{\circ}_{37\text{bulge loop}} = (-0.33 \cdot \Delta G^{\circ}_{37\text{duplex}}) - 0.7$ ($r^2 = 0.41$). Where $\Delta G^{\circ}_{37\text{bulge loop}}$ is the free energy increment (in kcal/mol) for insertion of a bulge loop into a duplex and $\Delta G^{\circ}_{37\text{duplex}}$ is the free energy of the duplex without the bulge. Finally, we compared the stability of the less stable duplex stem with the thermodynamic contribution of the bulge adjacent to a wobble base pair to helix formation (Figure 3c). A linear fit of the data for bulge loops adjacent to wobble base pairs in figure 3c gives the following: $\Delta G^{\circ}_{37\text{bulge loop}} = (-0.66 \cdot \Delta G^{\circ}_{37\text{less stable stem}}) + 0.0$ ($r^2 = 0.37$). This line

was not significantly different than the line for the bulge loops adjacent to Watson-Crick base pair, so both sets of data were combined. The linear fit for the combined data give the following: $\Delta G^{\circ}_{37\text{bulge loop}} = (-0.62 * \Delta G^{\circ}_{37\text{less stable stem}}) - 0.25$ ($r^2 = 0.38$). While the fit of the data in figure 3c is slightly better than the fit in figure 3b, the difference is so small as to be meaningless. So in considering the two relationships, we found using the less stable stem as more meaningful, because in Figure 3c, all of the less destabilizing bulge data points are now clustered. They all appear to be inserted adjacent to a stem that had a stability of less than 5 kcal/mol. These results are summarized in Table 6.

In an earlier report on bulge loops (15), non-nearest-neighbor interactions were observed for the thermodynamic of bulge loop insertion into a duplex. Substitution of a CG base pair for an AU base pair, two nucleotides removed from the bulge caused the bulge to be more destabilizing. It was also observed that the addition of a 3' dangling end also caused the bulge to have more of a destabilizing effect. Both of these observations are in concordance with the relationship described above. In both cases, substitution of a GC base pair for an AU base pair and the addition of a 3' dangling end increases the stability of the stem adjacent to the bulge and therefore should increase the destabilizing effect of the inserted bulge.

Similar non-nearest-neighbor effects have been observed with other structural motifs. In particular, there are several reports where non-nearest-neighbor effects have influenced the thermodynamics of single mismatches in RNA duplexes (42,43). The position of the single mismatch with a duplex has been shown to influence the stability of the duplex. As the bulge was moved closer to the terminus (decreasing the stability of the stem), the stability of the duplex increased. This effect was somewhat sequence specific as it was observed for UU and AA single mismatches but not for GG (42).

The influence of the adjacent stem on the thermodynamics of bulge loop insertion into an RNA helix may be related to the tight packing and electrostatic strain present in the RNA duplex (43). The lower the stability of the adjacent stem, the easier the structural perturbation from the insertion of the bulged nucleotide can be dissipated along the neighboring base pairs. Therefore, as the stability of the neighboring stem decreases, it becomes easier (less energetically costly) to insert a bulge loop, or other structural motif (e.g. single mismatch).

Nearest-Neighbor Influences on the Thermodynamics for Bulge Loops Adjacent to Wobble Base Pairs

In our analysis thus far, we have considered the bulge loops adjacent to wobble base pairs as a single group, but in fact, the position and orientation of the nearest-neighbor wobble base pair does influence thermodynamic of bulge loop formation. These influences are examined in figure 4, where the free energy increment for bulge loop formation is graphed as a function of the position and orientation of the wobble base pair in relation to the bulge. In figure 4, the free energy increment for bulge loop formation as a function of the less stable stem for each family of bulge loops is graphed relative to the least squares fit for all of the data points. For example,

if we focus on the bulge sequences of the type $\begin{pmatrix} 5' & U & B & X \\ 3' & G & & Y \end{pmatrix}$, all 10 of the bulges data points fall below the line by an average of 0.6 kcal/mol. Therefore, these bulges have a smaller destabilization on duplex formation than other bulge loops. This may be caused by the geometry of the GU base pair which produces a change in the twist angle of the RNA duplex (35). For

sequences of the type $\begin{pmatrix} 5' & U & X \\ 3' & G & Y \end{pmatrix}$, the twist angle between the base pairs is increased to about 40° which leads to unstacking of the wobble base pair with the adjacent base pair in the helix (Figure 3A). $\begin{pmatrix} 5' & U & X \\ 3' & G & Y \end{pmatrix}$ nearest-neighbor base pairs are among the less stable. For

sequences of the type $\begin{pmatrix} 5' & X & B & G \\ 3' & Y & & U \end{pmatrix}$, five of the seven bulges have values that fall above the line although the average is only 0.2 kcal/mol greater, within the error of the experiment.

For sequences of the type $\begin{pmatrix} 5' & G & B & X \\ 3' & U & & Y \end{pmatrix}$ and $\begin{pmatrix} 5' & X & B & U \\ 3' & Y & & G \end{pmatrix}$, 11 of the 15 bulges have values that fall above the line, indicating that they are more destabilizing than other bulges.

Excluding the very less destabilizing $\begin{pmatrix} 5' & G & U & G \\ 3' & U & & C \end{pmatrix}$ bulge (first value in Table 5), the average value is 0.4 kcal/mol above the line. In a similar analysis of the geometry of a $\begin{pmatrix} 5' & G & X \\ 3' & U & & Y \end{pmatrix}$ base pair, the wobble base pair decreases the twist angle between the base pairs (Figure 3B). In this instance, the base pair still stacks well with the wobble pair, and these nearest-neighbor pairs are among the more stable, so the bulge has a greater potential to disrupt the nearest-neighbor base pairs. For the bulges inserted between two wobble base pairs, all five of the data points fall below the line by an average of 0.6 kcal/mol. Consecutive wobble pairs also leads to unstacking of the bases as seen in Figure 3C. That a bulge between two adjacent wobble base pairs is the least destabilizing may be due to the fact that the tandem GU pairs are among the least stable nearest-neighbor base pair. In fact they contribute a positive free energy to duplex formation (36). These results are summarized in Table 4. The parameters in Table 4 can be combined with the nearest-neighbor parameters for duplex formation (32) to predict the thermodynamic stability of RNA duplexes containing bulge loops.

In Figure 4, five data points are circled, three that correspond to bulge loops that are significantly less destabilizing than predicted from the linear regression and two that are more destabilizing than predicted. The three sequences that are less destabilizing are:

$\begin{pmatrix} 5' & A & C & U & G & U & G & C & G \\ 3' & U & G & A & U & & C & G & C \end{pmatrix}$, $\begin{pmatrix} 5' & G & C & U & A & G & A & C \\ 3' & C & G & G & & C & U & G \end{pmatrix}$, and $\begin{pmatrix} 5' & G & A & C & A & U & A & G & U & C \\ 3' & C & U & G & & G & U & C & A & G \end{pmatrix}$.

There does not appear to be any common nearest-neighbor nor non-nearest-neighbor features that would explain their free energy increment. The position and orientation of the bulge is different in each case as well as the differences in the length and stability of the stems relative to the position of the bulge. In other sequence contexts, all three of the bulges have approximately the predicted value for the free energy increment of duplex destabilization. The two bulges that were circled as more destabilizing

than predicted have the sequences: $\begin{pmatrix} 5' & C & A & G & U & A & U & A & G & U & C \\ 3' & G & U & C & A & & G & U & C & A & G \end{pmatrix}$ and $\begin{pmatrix} 5' & C & A & G & U & G & U & A & G & U & C \\ 3' & G & U & C & A & & G & U & C & A & G \end{pmatrix}$.

In this case both bulges are within the same duplex context. Again, there is no obvious explanation for the larger free energy increment for these bulges.

Enthalpic Contributions of Group1 Single Nucleotide Bulge Loops to Duplex Stability

Since the free energy increment of the insertion of a bulge loop into a duplex was dependent upon the stability of the stem adjacent to the insertion, we investigated the influence of stem stability on the enthalpy of bulge loop insertion. Figure 6 displays the enthalpy of bulge loop insertion as a function of the stability of the less stable stem of the duplex for bulges adjacent to both Watson-Crick and wobble base pairs. The least squares fit for the Watson-Crick and wobble data were first considered separately.

Neither line had a slope significantly different than zero so the data sets were combined. The slope of the line for the combined Watson-Crick and wobble enthalpy values were again not significantly different than zero suggesting that the average enthalpy value is a reasonable approximation for the enthalpic energy contribution. The average enthalpic value for the combined data is 16.5 ± 11.4 kcal/mol. The enthalpy value can be used in conjunction with the free energy and enthalpy parameters for other nearest-neighbor motifs to determine the stability of RNA structures at temperatures other than 37 °C (34).

Phylogenetic Analysis of Single Nucleotide Bulge Loops

The database examined in this study contained 4330 group I single nucleotide bulge loops, 3520 closed with Watson-Crick and 810 closed wobble base pairs. The frequency of occurrence for the group I single nucleotide bulge loops are listed in Tables 3 and 6. For the Watson-Crick closed group I single nucleotide bulge loops, nearly 70 % of the total represent adenosine bulge loops. No other bulge sequence occurs more frequently than 4% except than (GUG/C C). Since the stability of group I single nucleotide bulge loops is independent of the identity of the bulge, there is no correlation between the thermodynamic contribution of the bulge and its frequency of occurrence. Therefore, the selection of naturally occurring bulge nucleotide sequences must be related to factors other than stability.

When the bulge has a wobble nearest neighbor, the position and orientation of the bulge does effect its contribution to stability. Nearly 90% of the naturally occurring bulged nucleotides are purine residues, with adenosine representing nearly 80%. The most frequent (76%) type of purine bulges have a 5' U/G, the more stable orientation; while the less stable 3' U/G represents less than 15% of the naturally occurring bulge sequences. However, the most stable bulge loop (with two adjacent wobble base pairs) represent less than 2% of the naturally occurring sequences and several bulge combinations were not observed in the database.

Single Nucleotide Bulge Loops in Natural Contexts

The effect of stem stability on the influence of single nucleotide bulge loop on duplex formation is particularly important to the analysis of naturally occurring RNAs where the average duplex is less than 7 nucleotides. In fact, of the 20 single nucleotide bulge loops found in the small and large *E. coli* ribosomal RNA (33), 19 have a stem with stability less than 5 kcal/mol. The average stability for the less stable stem is approximately 3 kcal/mol, excluding the influence of terminal mismatches. Therefore, because of the low stability of duplex stems in natural RNAs, the influence of single nucleotide bulge loops on duplex stability is less than previously thought (16).

Although the experiments from this and previous bulge loops studies (15,16) are by agreement performed at 1M NaCl and show that bulges are generally destabilizing to double-stranded regions of RNA. The conformations of bulged nucleotides can afford them stabilization through binding of other biologically relevant ligands. Bulges can be stabilized via either direct or water-mediated interactions with divalent cations (42), often within the context of tertiary interactions (43-46). Examples include interactions of the A-rich bulge of P4-P6 of the group I intron (43), metal binding in the bulge region of HIV-1 TARN NRA (44,45), or within the bulged region of the leadzyme (46). In addition, bulges function as critical portions of recognition elements for RNA-protein interactions (47-50). Thus, the destabilization of double stranded RNA by bulge loops is often necessary in order for RNA to properly fold into its functional structures or form RNA-protein complexes which serve to offset the destabilization of the secondary structure.

Supplementary Material

Refer to Web version on PubMed Central for supplementary material.

References

1. Schuwirth BS, Borovinskaya MA, Hau CW, Zhang W, Vila-Sanjurjo A, Holton JM, Cate JH. Structures of the bacterial ribosome at 3.5 Å resolution. *Science* 2005;310:827–834. [PubMed: 16272117]
2. Allen GS, Zavialov A, Gursky R, Ehrenberg M, Frank J. The cryo-EM structure of a translation initiation complex from *Escherichia coli*. *Cell* 2005;121:703–712. [PubMed: 15935757]
3. Korostelev A, Trakhanov S, Laurberg M, Noller HF. Crystal structure of a 70S ribosome-tRNA complex reveals functional interactions and rearrangements. *Cell* 2006;126:1065–1077. [PubMed: 16962654]
4. Doudna JA, Cech TR. The chemical repertoire of natural ribozymes. *Nature* 2002;418:222–228. [PubMed: 12110898]
5. Fedor MJ, Williamson JR. The catalytic diversity of RNAs. *Nat Rev Mol Cell Biol* 2005;6:399–412. [PubMed: 15956979]
6. Lilley DM. Structure, folding and mechanisms of ribozymes. *Curr Opin Struct Biol* 2005;15:313–323. [PubMed: 15919196]
7. Bevilacqua PC, Yajima R. Nucleobase catalysis in ribozyme mechanism. *Curr Opin Chem Biol* 2006;10:455–464. [PubMed: 16935552]
8. Tucker BJ, Breaker RR. Riboswitches as versatile gene control elements. *Curr Opin Struct Biol* 2005;15:342–348. [PubMed: 15919195]
9. Gilbert SD, Montange RK, Stoddard CD, Batey RT. Structural Studies of the Purine and SAM Binding Riboswitches. *Cold Spring Harb Symp Quant Biol* 2006;71:259–268. [PubMed: 17381305]
10. Sashital DG, Butcher SE. Flipping off the riboswitch: RNA structures that control gene expression. *ACS Chem Biol* 2006;1:341–345. [PubMed: 17163768]
11. Brion P, Westhof E. Hierarchy and dynamics of RNA folding. *Annu Rev Biophys Biomol Struct* 1997;26:113–137. [PubMed: 9241415]
12. Tinoco I Jr, Bustamante C. How RNA folds. *J Mol Biol* 1999;293:271–281. [PubMed: 10550208]
13. Mathews DH, Sabina J, Zuker M, Turner DH. Expanded sequence dependence of thermodynamic parameters improves prediction of RNA secondary structure. *J Mol Biol* 1999;288:911–940. [PubMed: 10329189]
14. Mathews DH, Disney MD, Childs JL, Schroeder SJ, Zuker M, Turner DH. Incorporating chemical modification constraints into a dynamic programming algorithm for prediction of RNA secondary structure. *Proc Natl Acad Sci U S A* 2004;101:7287–7292. [PubMed: 15123812]
15. Longfellow CE, Kierzek R, Turner DH. Thermodynamic and spectroscopic study of bulge loops in oligoribonucleotides. *Biochemistry* 1990;29:278–285. [PubMed: 2322546]
16. Znosko BM, Silvestri SB, Volkman H, Boswell B, Serra MJ. Thermodynamic Parameters for an Expanded Nearest-Neighbor Model for the Formation of RNA Duplexes with Single Nucleotide Bulges. *Biochemistry* 2002;41:10406–10417. [PubMed: 12173927]
17. Harper JW, Logsdon NJ. Refolded HIV-1 tat protein protects both bulge and loop nucleotides in TAR RNA from ribonucleolytic cleavage. *Biochemistry* 1991;30:8060–8066. [PubMed: 1868081]
18. Rounseville MP, Kumar A. Binding of a host cell nuclear protein to the stem region of human immunodeficiency virus type 1 trans-activation-responsive RNA. *J Virol* 1992;66:1688–1694. [PubMed: 1738206]
19. Rounseville MP, Lin HC, Agbottah E, Shukla RR, Rabson AB, Kumar A. Inhibition of HIV-1 replication in viral mutants with altered TAR RNA stem structures. *Virology* 1996;216:411–417. [PubMed: 8607271]
20. Klasens BI, Thiesen M, Virtanen A, Berkhout B. The ability of HIV-1 AAUAAA signal to bind polyadenylation factors is controlled by local RNA structure. *Nucleic Acids Res* 1999;27:446–454. [PubMed: 9862964]
21. Woese CR, Gutell RR. Evidence for several higher order structural elements in ribosomal RNA. *Proc Natl Acad Sci U S A* 1989;86:3119–3122. [PubMed: 2654936]

22. Lanciault C, Champoux JJ. Effects of unpaired nucleotides within HIV-1 genomic secondary structures on pausing and strand transfer. *J Biol Chem* 2005;280:2413–2423. [PubMed: 15542863]
23. Usman N, Ogilvie KK, Jiang M-V, Cedergren R. *J Am Chem Soc* 1987;109:7845–7854.
24. Wincott F, DiRenzo A, Shaffer C, Grimm S, Tracz D, Workman C, Sweedler D, Gonzalez C, Scaringe S, Usman N. Synthesis, deprotection, analysis and purification of RNA and ribozymes. *Nucleic Acids Res* 1995;23:2677–2684. [PubMed: 7544462]
25. Borer, PN. *Handbook of Biochemistry and Molecular Biology: Nucleic Acids*. Fasman, GD., editor. CRC Press; Cleveland OH: 1975. p. 589
26. Richards, EG. *Handbook of Biochemistry and Molecular Biology: Nucleic Acids*. Fasman, GD., editor. CRC Press; Cleveland OH: 1975. p. 197
27. Serra MJ, Axenson TJ, Turner DH. A Model for the Stabilities of RNA Hairpins Based on a Study of the Sequence Dependence of Stability for Hairpins of Six Nucleotides. *Biochemistry* 1994;33:14289–14296. [PubMed: 7524674]
28. McDowell JA, Turner DH. Investigation of the Structural Basis for Thermodynamic Stabilities of Tandem GU Mismatches: Solution Structure of (rGAGGUCUC)₂ by Two-Dimensional NMR and Simulated Annealing. *Biochemistry* 1996;35:14077–14089. [PubMed: 8916893]
29. Borer P, Dengler B, Tinoco I Jr. Stability of Ribonucleic acid Double-stranded Helices. *J Mol Biol* 1974;86:843–853. [PubMed: 4427357]
30. Freier SM, Kierzek R, Jaeger JA, Sugimoto N, Caruthers MH, Neilson T, Turner DH. Improved free-energy parameters for predictions of RNA duplex stability. *Proc Natl Acad Sci U S A* 1986;83:9373–9377. [PubMed: 2432595]
31. Allawi HT, SantaLucia J Jr. Thermodynamics and NMR of internal G.T mismatches in DNA. *Biochemistry* 1997;36:10581–10594. [PubMed: 9265640]
32. Xia T, SantaLucia J Jr, Burkard ME, Kierzek R, Schroeder SJ, Jiao X, Cox C, Turner DH. Thermodynamic parameters for an expanded nearest-neighbor model for formation of RNA duplexes with Watson-Crick base pairs. *Biochemistry* 1998;37:14719–14735. [PubMed: 9778347]
33. Cannone JJ, Subramanian S, Schnare MN, Collett JR, D'Souza LM, Du Y, Feng B, Lin N, Madabusi LV, Muller KM, Pande N, Shang Z, Yu N, Gutell RR. The comparative RNA web (CRW) site: an online database of comparative sequence and structure information for ribosomal, intron, and other RNAs. *BMC Bioinformatics* 2002;3:2. [PubMed: 11869452]
34. Lu ZJ, Turner DH, Mathews DH. A set of nearest neighbor parameters for predicting the enthalpy change of RNA secondary structure formation. *Nucleic Acids Res* 2006;34:4912–4924. [PubMed: 16982646]
35. Masquida B, Westhof E. On the wobble GoU and related pairs. *RNA* 2000;6:9–15. [PubMed: 10668794]
36. He L, Kierzek R, Santa Lucia J Jr, Walter AE, Turner DH. Nearest Neighbor Parameters for GU Mismatches: GU/UG Is Destabilizing in the Context CGUG/GUGC UGUA/AUGA, and AGUU/UUGA but Stabilizing in GGUC/CUGG. *Biochemistry* 1991;30:11124–11132. [PubMed: 1718426]
37. Mathews DH, Sabina J, Zuker M, Turner Douglas H. Expanded Sequence Dependence of Thermodynamic Parameters Improves Prediction of RNA Secondary Structure. *J Mol Bio* 1999;288:911–940. [PubMed: 10329189]
38. Wu M, McDowell JA, Turner DH. A periodic table of symmetric tandem mismatches in RNA. *Biochemistry* 1995;34:3204–3211. [PubMed: 7533535]
39. Schroeder SJ, Turner DH. Factors affecting the thermodynamic stability of small asymmetric internal loops in RNA. *Biochemistry* 2000;39:9257–9274. [PubMed: 10924119]
40. Masquida B, Sauter C, Westhof E. A sulfate pocket formed by three GU pairs in the 0.97 Å resolution X-ray of a nonameric RNA. *RNA* 1999;5:99–112.
41. Trikha J, Filman DJ, Hogle JM. Crystal structure of a 14 bp RNA duplex with non-symmetrical tandem GxU wobble base pairs. *Nucleic Acids Res* 1999;27:1728–1739. [PubMed: 10076005]
42. Xiong Y, Deng J, Sudarsanakumar C, Sundaralingam M. Crystal structure of an RNA duplex r (gugucgac)₂ with uridine bulges. *J Mol Biol* 2001;313:573–582. [PubMed: 11676540]
43. Cate JH, Gooding AR, Podell E, Zhou K, Golden BL, Kundrot CE, Cech TR, Doudna JA. RNA tertiary structure mediation by adenosine platforms. *Science* 1999;273:1678–1685. [PubMed: 8781224]

44. Ippolito JA, Steitz TA. A 1.3-Å resolution crystal structure of the HIV-1 trans-activation response region RNA stem reveals a metal ion-dependent bulge conformation. *Proc Natl Acad Sci U S A* 1998;95:9819–9824. [PubMed: 9707559]
45. Olejniczak M, Gdaniec Z, Fischer A, Grabarkiewicz T, Bielecki L, Adamiak RW. The bulge region of HIV-1 TAR RNA binds metal ions in solution. *Nucleic Acids Res* 2002;30:4241–4249. [PubMed: 12364603]
46. Wedekind JE, McKay DB. Crystal structure of the leadzyme at 1.8 Å resolution: metal ion binding and the implications for catalytic mechanism and allo site ion regulation. *Biochemistry* 2003;42:9554–9563. [PubMed: 12911297]
47. Jaffrey SR, Haile DJ, Klausner RD, Harford JB. The interaction between the iron-responsive element binding protein and its cognate RNA is highly dependent upon both RNA sequence and structure. *Nucleic Acids Res* 1993;21:4627–4631. [PubMed: 8233801]
48. Valegard K, Murray JB, Stonehouse NJ, van den Worm S, Stockley PG, Liljas L. The three-dimensional structures of two complexes between recombinant MS2 capsids and RNA operator fragments reveal sequence-specific protein-RNA interactions. *J Mol Biol* 1997;270:724–738.
49. Lim F, Peabody DS. RNA recognition site of PP7 coat protein. *Nucleic Acids Res* 2002;30:4138–4144. [PubMed: 12364592]
50. Seto AG, Livengood AJ, Tzfati Y, Blackburn EH, Cech TR. A bulged stem tethers Est1p to telomerase RNA in budding yeast. *Genes Dev* 2002;16:2800–2812. [PubMed: 12414733]

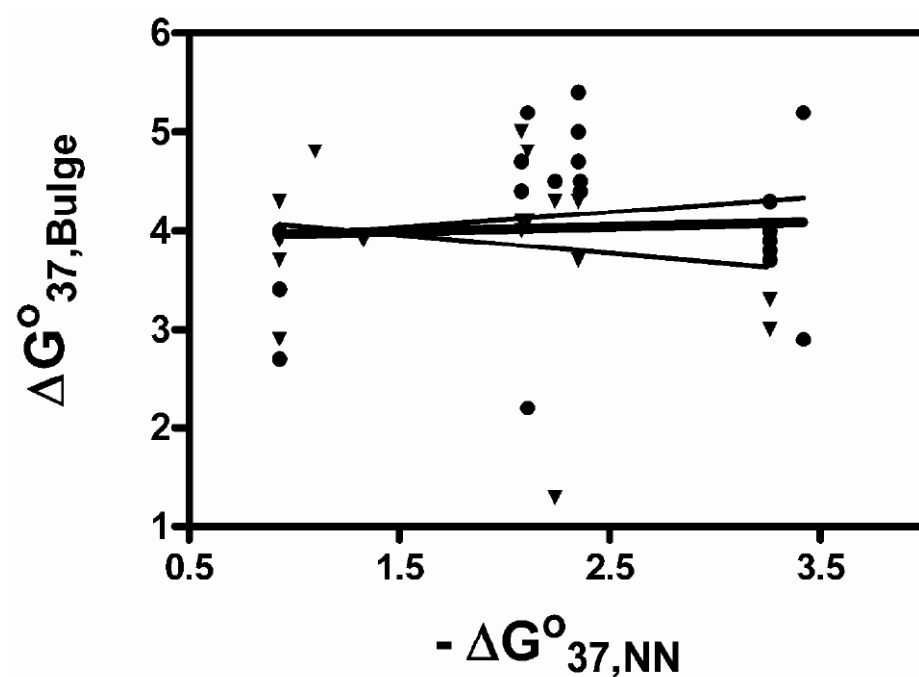


Figure 1. Plot of free energy change for bulge loop formation, $\Delta G^{\circ}_{37bulge}$, vs the free energy increment, ΔG°_{37nn} , for the Watson-Crick nearest-neighbor interaction at the site of the bulge. Energy differences between purine (●) and pyrimidine (▼) bulge loops. Thin solid lines are the linear regression lines for the purine and pyrimidine data. Dark solid line is the linear regression for all data points.

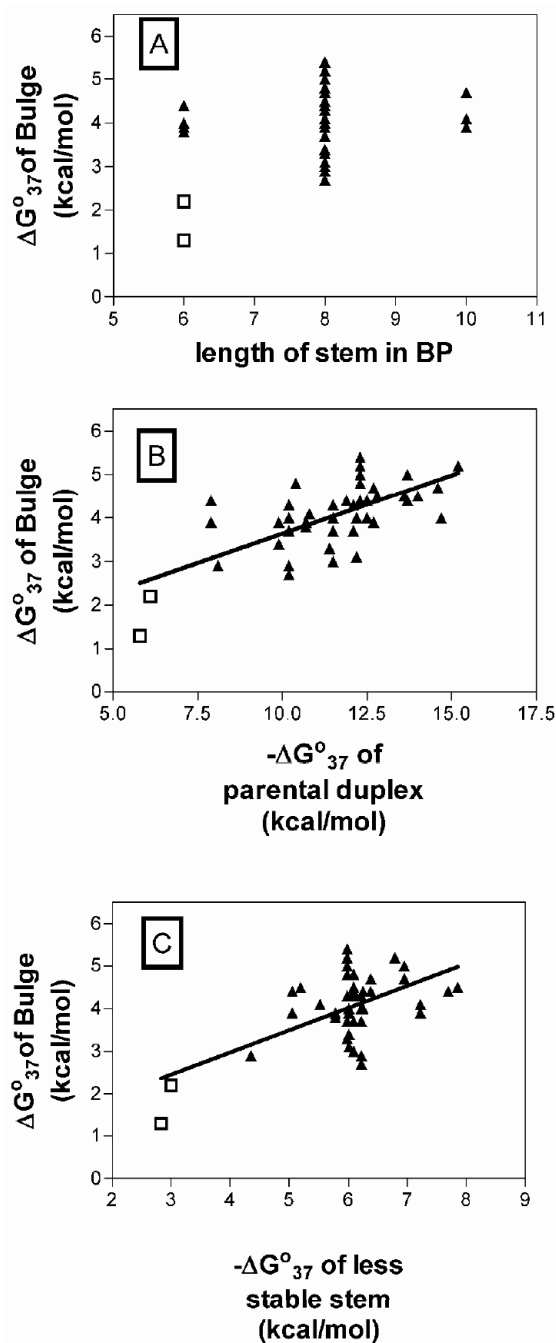


Figure 2.

Panel A. Plot of free energy change for bulge loop formation, $\Delta G^{\circ}_{37\text{bulge}}$, vs length of the duplex. Panel B. Plot of free energy change for bulge loop formation, $\Delta G^{\circ}_{37\text{bulge}}$, vs free energy of parental duplex. Panel C. Plot of free energy change for bulge loop formation, $\Delta G^{\circ}_{37\text{bulge}}$, vs free energy of less stable duplex stem (Note, stem free energy was calculated without the inclusion of the free energy of duplex initiation.). Bulge loops adjacent to Watson-Crick nearest neighbors (\blacktriangle) and “red” bulge loops from Table 3 (\square). Lines are the least-squares fit of the data points.

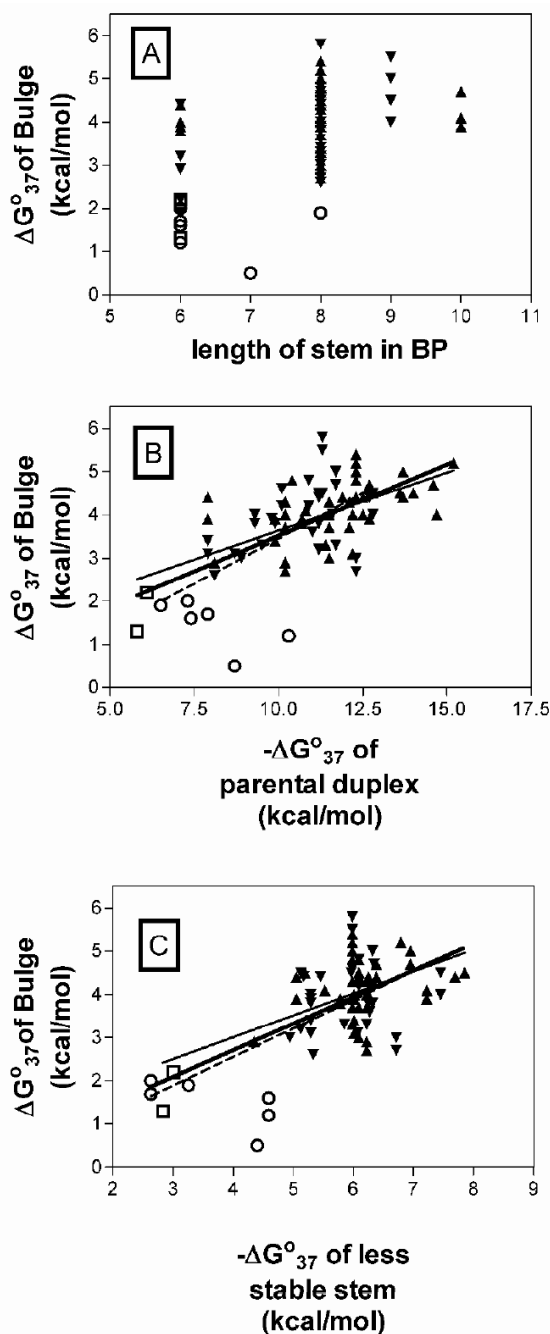
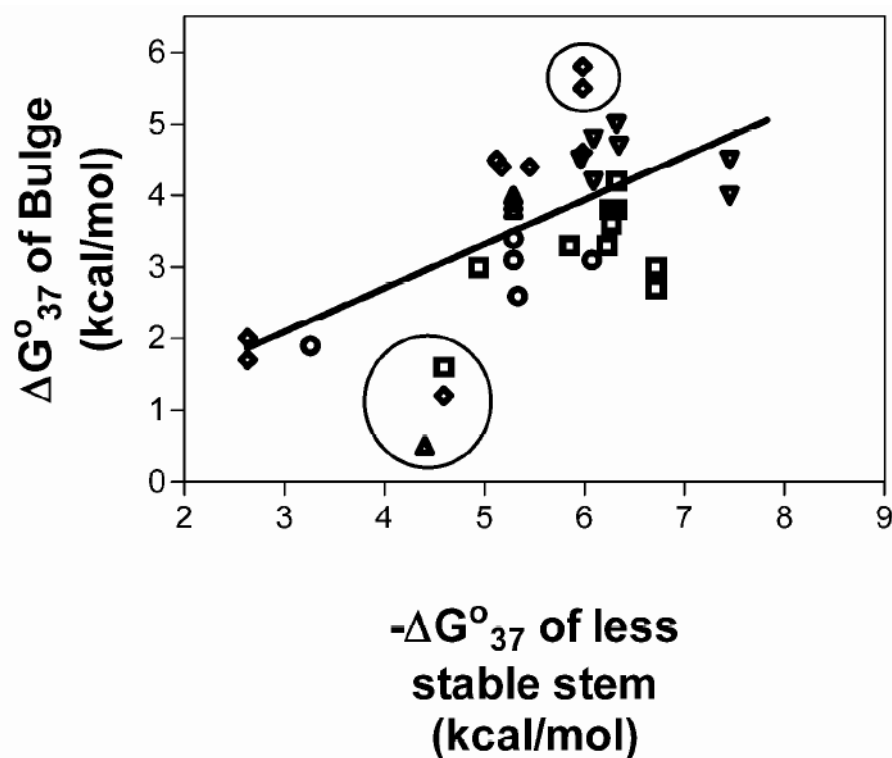


Figure 3.

Panel A. Plot of free energy change for bulge loop formation, $\Delta G^{\circ}_{37\text{bulge}}$, vs length of the duplex. Panel B. Plot of free energy change for bulge loop formation, $\Delta G^{\circ}_{37\text{bulge}}$, vs free energy of parental duplex. Panel C. Plot of free energy change for bulge loop formation, $\Delta G^{\circ}_{37\text{bulge}}$, vs free energy of less stable duplex stem (Note, stem free energy was calculated without the inclusion of the free energy of duplex initiation.). Bulge loops adjacent to Watson-Crick nearest neighbors (∇), bulge loops adjacent to wobble nearest neighbors (\circ), and "red" bulge loops from Tables 3 (\square) and 6 (\diamond). Lines are the least-squares fit of the data points.

**Figure 4.**

Panel A. Plot of free energy change for bulge loop formation, $\Delta G^{\circ}_{37\text{bulge}}$, vs free energy of parental duplex. Panel B. Plot of free energy change for bulge loop formation, $\Delta G^{\circ}_{37\text{bulge}}$, vs free energy of less stable duplex stem (Note, stem free energy was calculated without the

inclusion of the free energy of duplex initiation.). $\begin{pmatrix} 5' & U & B & X \\ 3' & G & & Y \end{pmatrix}$ bulge loops (\square), $\begin{pmatrix} 5' & G & B & X \\ 3' & U & & Y \end{pmatrix}$ bulge loops (\diamond), $\begin{pmatrix} 5' & X & B & G \\ 3' & Y & & U \end{pmatrix}$ bulge loops (\triangle), $\begin{pmatrix} 5' & X & B & U \\ 3' & Y & & G \end{pmatrix}$ bulge loops (\circ), and double GU bulge loops (\circ). Lines are the linear regression for all Watson-Crick and wobble base pair data points.

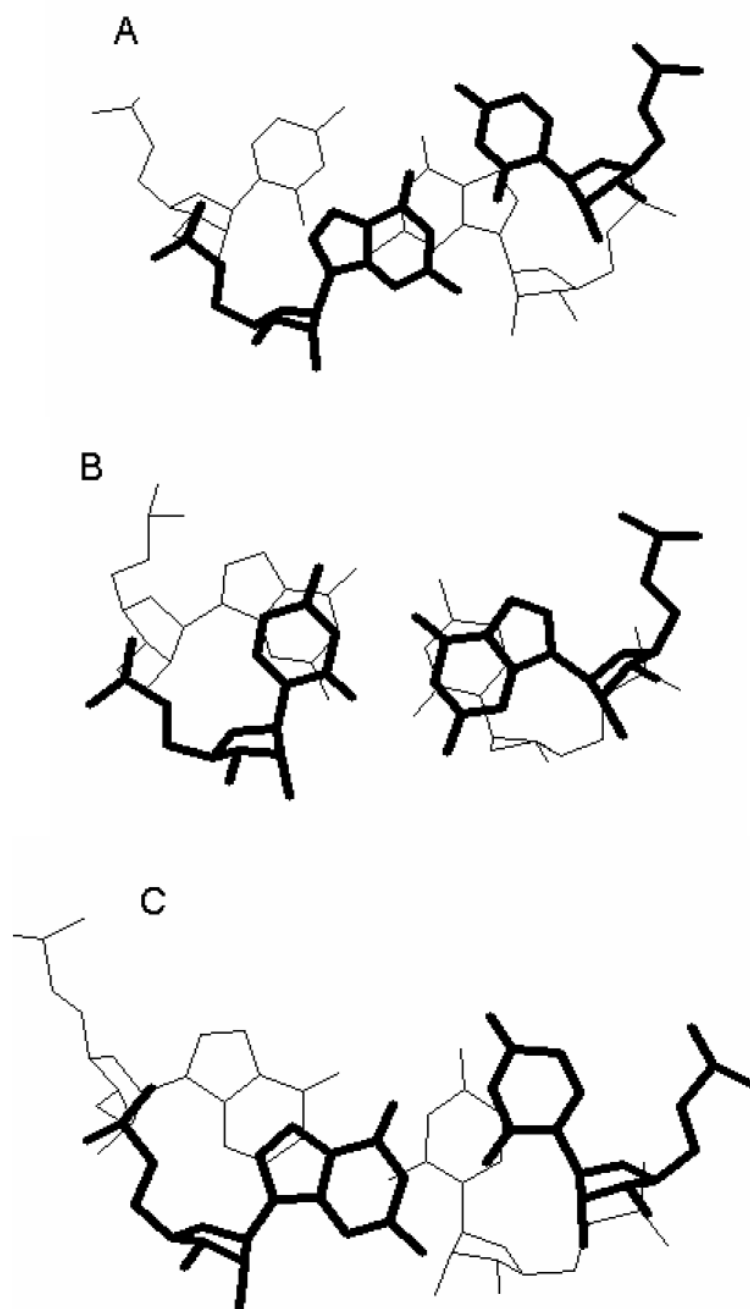


Figure 5. Stacking of wobble GU base pairs. Panel A, view down the helix axis of 5'UG/3'GC. Panel B, view down helix axis of 5'GU/3'CG. Panel C, view down helix axis of 5'GG/3'UU. The wobble base pairs are shown as the nearer base pair and are drawn in bold. Examples are taken from the crystal structure of [r(CGUGAUCG)dC]₂ (40) panels A and B and (GGUAUUGCGGUACC)₂ (41).

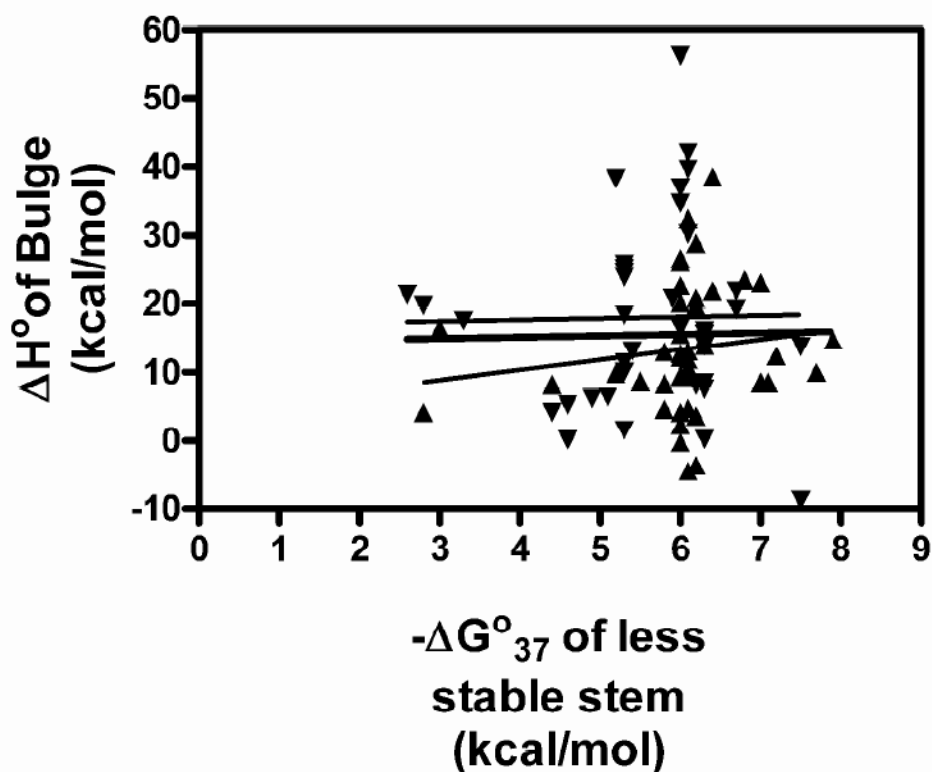


Figure 6.

Plot of enthalpy change for bulge loop formation, $\Delta H^\circ_{\text{bulge}}$, vs free energy of less stable duplex stem (Note, stem free energy was calculated without the inclusion of the free energy of duplex initiation.). Bulges adjacent to Watson-Crick nearest neighbors (▼), wobble nearest neighbors (▲). Lines are the linear regression for Watson-Crick and wobble base pair data points

Table 1

Examples of different classes of single nucleotide bulge loops

sequence	Potential bulge positions		Duplex sequence ($-\Delta G^{\circ}_{37}$)	
Group I				
CGCAGCC GCG CGG	CGCAGCC GCG CGG		CGCGCC (10.7) GCGCGG	
Group II				
CGCCGCC GCG CGG	CGCCGCC GCG CGG	CGCCGCC GC GCGG	CGCGCC (10.7) GCGCGG	CGCGCC (10.7) GCGCGG
Group III				
CGCUGCC GCG CGG	CGCUGCC GCG CGG	CGCUGCC GC GCGG	CGCGCC (10.7) GCGCGG	CGUGCC (8.9) GCGCGG
Group IV				
CGCCUGG GCG GCC	CGCCUGG GCG GCC	CGCCUGG GC GGCC	CGCUGG (8.5) GCGGCC	CGCUGG (8.5) GCGGCC
	CGCCUGG GCGG CC		CGCCGG (10.6) GCGGCC	

Table 2

Thermodynamic Parameters for Duplex Formation for Oligonucleotides Containing a Group I Single Nucleotide Bulge Adjacent to Watson-Crick Base Pairs^{d/}

oligomers ^b	T _M ⁻¹ vs log C _T plots				average of curve fits			
	-ΔH° (kcal/mol)	-ΔS° (eu)	-ΔG° ₃₇ (kcal/mol)	T _M ^c (°C)	-ΔH° (kcal/mol)	-ΔS° (eu)	-ΔG° ₃₇ (kcal/mol)	T _M ^c (°C)
Group I Purine								
GGCG A UCUG CCGC GAGC	60.2	162.3	9.9	55.4	60.5	163.0	10.0	55.8
GAGC A GUUC CUCG CCAG	65.2	180.3	9.3	50.8	69.5	193.2	9.6	51.2
GGCG A UUC CCGC AAGG	66.6	185.0	9.2	49.9	70.9	198.6	9.3	49.6
GGCG A UUC CCGC AAGC	67.6	191.3	8.3	45.4	66.0	186.0	8.3	45.6
GACCG A GC CUGG AUUG	54.5	149.9	8.0	45.4	56.1	155.2	8.0	45.4
GUGC A UGAG CACG ACUC	64.8	183.5	7.9	43.7	65.3	184.8	8.0	43.9
CAGUG A GC GUCA GUCG	48.5	133.1	7.3	41.8	52.3	144.7	7.4	42.5
CAGU A GAG GUCA CUCG	59.1	167.8	7.1	39.9	63.5	181.7	7.1	39.8
CAGU A CAG GUCA GUCG	52.8	148.0	6.9	39.4	49.2	136.4	6.9	39.6
GUGUGUG CACA ACAC	54.6	155.2	6.4	36.4	58.4	167.1	6.5	37.0
GAG A CAC CUC GUG	45.0	127.9	5.3	28.6	50.7	146.8	5.2	29.1
GAU A GAC CUA CUG	37.4	108.5	3.8	15.7	34.8	99.1	4.1	16.6
Group I Pyrimidine								
GGCAUG A GC CCGU CUGC	53.7	145.3	8.7	49.9	60.4	166.5	8.8	49.0
GACAUG G GC CUGU CACG	67.7	181.3	8.5	46.7	57.9	159.7	8.4	47.1
CAGG U AAGC GUCC UUCG	72.6	207.0	8.4	45.1	78.5	225.7	8.5	45.0
CACAUG G CAC GUGU CGUG	61.3	171.2	8.2	45.6	64.8	182.4	8.3	45.6
CACAC G CAC GUGU CGUG	47.8	127.9	8.1	47.6	58.8	162.9	8.3	46.8
CAGG C AAGC GUCC UUCG	62.3	175.9	7.8	43.3	69.5	198.4	7.9	43.3
GACG C UAGC CUGC AUUG	37.8	97.6	7.6	45.8	35.9	91.1	7.6	46.5
CAGUC G AGC GUCA CUCG	56.7	158.8	7.5	42.4	57.0	159.4	7.6	43.0
GCAUC G UG CGUA ACAC	65.7	192.6	6.0	34.4	66.2	194.1	6.0	34.7
CAGAC U AGC GUCU AUUG	43.6	122.6	5.6	30.4	35.9	97.6	5.7	29.6
GUG C UUC CAC AAG	44.5	129.1	4.4	23.0	44.9	130.0	4.6	24.0

^aSolutions are 1.0 M NaCl, 10 mM sodium cacodylate, 0.5 mM EDTA pH 7.

^bNucleotide in bold is the bulge residue. Top sequence is written 5' → 3'.

^cCalculated at 10⁻⁴ M oligomer concentration.

Table 3
Thermodynamic Parameters and natural occurrence for single nucleotide Group I bulges closed by Watson-Crick base pairs

bulge sequence ^d	$\Delta G^{\circ}_{37\text{bulge}}$	b (kcal/mol)	$\Delta H^{\circ}_{\text{bulge}}$ (kcal/mol)	Percentage of naturally occurring group I sequences ^e	bulge sequence ^d	$\Delta G^{\circ}_{37\text{bulge}}$ (kcal/mol) ^b	$\Delta H^{\circ}_{\text{bulge}}$ (kcal/mol)	Percentage of naturally occurring group I sequences ^e
A bulges								
CAC G G	3.9 4.3 ^{dc}		4.7 ^d 13.1 ^c	12.8	UCA A U	3.9 ^c	8.5 ^c	1.8
GAG C C	3.8 3.7 ^{dc}		8.3 ^d 9.4 ^c	11.4	GCG C C	3.0 ^c	-4.5 ^c	1.5
CAG G C	4.5 4.4 ^c		14.7 10.0 ^c	10.6	UCU A A	3.9 2.9 ^c	4.2 19.7 ^c	1.0
CAU G A	4.4 4.4 ^c		11.9 13.9 ^c	10.4	ACA U U	4.3 ^c	-3.7 ^c	0.9
UAC A G	5.4 4.7 ^c		26.0 8.5 ^c	9.9	ACG U C	4.0 4.1 ^c	22.6 12.4 ^c	0.7
GAC C G	2.9 5.2		8.2 23.4	8.2	UCG A C	4.8 4.1 ^c	20.1 8.7 ^c	0.7
GAU C A	4.5 4.5		9.8 10.6	2.8	ACU U A	4.8	32.4	0.4
UAU A A	4.0 ^c		20.8 ^c	1.5	GCA C U	4.3	9.4	0.4
UAG A C	2.2 5.2		16.4 15.6	1.2	GCU C A	1.3 4.3	4.2 38.5	0.3
G bulges								
CGC G G	4.0 ^c		8.8 ^c	1.9	GUG C C	3.9 3.3 ^{dc}	13.0 ^d 2.3 ^c	12.3
UGCA G	5.0		26.6	1.1	AUG U C	4.0 4.0 5.0	15.1 12.8 23.0	3.2
CGU G A	4.7		21.8	0.3	AUA U U	3.7 ^c	3.7 ^c	3.0
UGU A A	3.4 2.9 ^c		12.2 28.8 ^c	0.2	GUA C U	3.7	-0.3	1.6

^aTop strand is written 5→3'.

^bValues calculated as described in text.

^c(16)

^d(15)

^eTotal number of single nucleotide group I bulge sequences closed by Watson-Crick base pairs is 3520.

Thermodynamic Parameters for Duplex Formation for Oligonucleotides Containing a Group I Single Nucleotide Bulge Adjacent to GU Wobble Base Pairs^{ad}

Table 4

oligomers ^b	T _M ⁻¹ vs log C _T plots				average of curve fits			
	-ΔH° (kcal/mol)	-ΔS° (eu)	-ΔG° ₃₇ (kcal/mol)	T _M ^c (°C)	-ΔH° (kcal/mol)	-ΔS° (eu)	-ΔG° ₃₇ (kcal/mol)	T _M ^c (°C)
purine bulges with 5' adjacent G-U pairs								
CGGUGCAGC GCCG GUGC	52.7	139.1	9.6	55.8	51.2	134.1	9.6	57.0
CGGUACAGC GCCG GUGC	55.3	148.3	9.3	53.2	53.8	143.7	9.3	53.6
CAGUAGACG GUCG CUGC	56.4	158.0	7.4	41.7	68.5	197.2	7.4	40.8
GCUUACGAC CGAG CUGC	79.2	231.6	7.4	40.3	75.2	218.8	7.3	40.3
GCUUAUUGG CGAG AACG	43.2	119.2	6.3	35.0	52.3	149.0	6.1	34.7
GUCUGUCAC CAGG AGUG	58.6	169.1	6.1	34.9	64.2	187.2	6.1	35.0
GCUUGUACC CGAG AUGG	53.5	153.6	5.8	33.0	59.5	173.0	5.9	33.5
GCUAGAC CGG CUG	49.9	142.1	5.8	32.7	55.6	160.5	5.8	32.9
purine bulges with 3' adjacent G-U pairs								
GACAUAGUC CUG GUCAG	73.6	207.6	9.2	48.8	63.1	174.4	9.0	49.4
CGGCAUACG GCCG GUGC	40.2	103.2	8.2	50.5	36.3	90.0	8.4	53.6
GUCGAUCAC CAGC GGUG	61.4	175.5	6.9	39.1	59.6	169.7	6.9	39.1
CAAGAUAGUC GUUC GUCAG	76.9	226.4	6.7	37.7	66.1	191.3	6.8	38.1
GGCGUAC CCG GUG	34.0	89.6	6.2	34.0	37.0	99.5	6.2	34.0
CAGUGUAGUC GUCA GUCAG	28.0	72.0	5.7	27.8	25.1	62.0	5.9	29.5
GCUUGUACC CGAA GUGG	57.2	167.1	5.4	31.0	56.1	162.9	5.6	31.9
CAGUAUAGUC GUCA GUCAG	49.3	141.8	5.3	29.6	42.7	119.7	5.6	30.4
GCGAUAG CGC GUC	34.5	95.3	5.0	23.4	26.9	69.0	5.5	25.5
purine bulges with both 5' and 3' adjacent G-U pairs								
GCUUGUACC CGAG GUGG	49.4	140.9	5.6	31.7	49.8	142.6	5.6	31.5
GUGUAUGUG CACG GCAC	50.8	146.2	5.5	30.8	55.8	162.7	5.4	30.7
GAUGUUAGC CUG GAUCG	54.0	160.3	4.3	24.9	45.7	131.6	4.8	26.0
pyrimidine bulges with 5' adjacent G-U pairs								
ACUGUGCG UGAU CGC	54.4	148.9	8.2	46.9	55.7	153.2	8.2	46.6
CAGGCGAGC GUCU CUUG	68.5	196.6	7.6	41.7	59.9	168.8	7.6	42.5
CAGGUGAGC GUCU CUUG	74.3	214.9	7.6	41.5	73.6	212.8	7.65	41.8
CAGGCUAGC GUCU AUUG	42.8	119.1	5.8	31.9	41.7	115.3	6.0	32.7
CAGGCAAGC GUCU UUCG	44.4	125.6	5.5	30.0	45.4	128.6	5.6	30.4
CAGGUAGC GUCU UUCG	61.1	180.0	5.3	30.9	60.2	176.6	5.4	31.4
pyrimidine bulges with 3' adjacent G-U pairs								
CAGGUGAGUC GUCC UUCAG	86.5	250.9	8.7	45.0	103.5	305.0	8.9	44.3
CAGGCGAGUC GUCC UUCAG	74.8	214.1	8.4	44.8	70.1	199.1	8.3	45.1
CAGGUGAGC GUCC UUCG	61.9	176.8	7.0	39.6	61.3	174.8	7.0	39.6

oligomers ^b	T _M ⁻¹ vs log C _T plots				average of curve fits			
	-ΔH° (kcal/mol)	-ΔS° (eu)	-ΔG° ₃₇ (kcal/mol)	T _M ^c (°C)	-ΔH° (kcal/mol)	-ΔS° (eu)	-ΔG° ₃₇ (kcal/mol)	T _M ^c (°C)
CAGUCGAGUC GUCA UUCAG	46.4	127.6	6.8	38.8	50.2	140.4	6.7	37.7
CAGGCCGAGC GUCC UUCG	58.9	168.0	6.7	38.1	63.4	183.0	6.7	37.8
CAGACGAGUC GUCU UUCAG	40.5	109.2	6.6	27.7	40.4	108.4	6.8	38.7
CAGAUAGAGUC GUCU UUCAG	37.5	101.4	6.0	32.9	38.8	105.0	6.2	34.5
Pyrimidine bulges with both 5' and 3' adjacent G-U pairs								
CAGGCCGAGC GUCU UUCG	52.5	153.3	4.9	27.8	54.6	160.8	4.7	27.0
CAGGUAGAGC GUCU UUCG	50.6	148.4	4.6	25.9	54.7	161.8	4.5	26.0

^a Solutions are 1.0 M NaCl, 10 mM sodium cacodylate, 0.5 mM EDTA pH 7.

^b Nucleotide in bold is the bulge residue. Top sequence is written 5' → 3'.

^c Calculated at 10⁻⁴ M oligomer concentration.

Table 5
Thermodynamic Parameters and natural occurrence for single nucleotide Group I bulges closed by GU base pairs

Bulge sequence ^d	$\Delta G^{\circ}_{37\text{bulge}}$ (kcal/mol)	$\Delta H^{\circ}_{\text{bulge}}$ (kcal/mol)	Percentage of naturally occurring group I sequences ^c	bulge sequence ^d	$\Delta G^{\circ}_{37\text{bulge}}$ (kcal/mol)	$\Delta H^{\circ}_{\text{bulge}}$ (kcal/mol)	Percentage of naturally occurring group I sequences ^c
Bulges with 5' G/U							
GUG U C	0.5 4.0	4.2 1.6	2.1	GUG C U	4.7 4.0	15.6 -8.8	2.2
GUA U U	4.0	10.0	0.6	AUG U U	4.8	42.0	1.1
GCA U U	3.8	25.8	0	GCG C U	5.0 4.5	16.1 13.7	1.0
GCU U A	3.9	25.2	0.0	UCG A U	4.5	34.6	0.6
GCG U C	4.0	11.4	0.0	ACG U U	4.2	39.7	0.1
Bulges with 5' U/G							
UAC G G	3.0 ^d , 3.0 3.8	6.2 ^d , 19.3 0.2	37.9	GAU C G	2.0, 4.4 4.5	21.3, 13.1 6.5	10.1
UAG G C	1.6, 3.6 3.3 ^d	0.1, 7.5 8.1 ^d	23.0	CAU G G	4.4 1.2	38.2 5.3	2.6
UGC G G	2.7	21.8	8.5	UAU A G	5.8	36.8	0.7
UAU G A	3.3	20.7	4.8	CGU G G	1.7	19.7	0.6
UGU G A	4.2 3.8	13.8 8.4	2.0	UGU A G	5.5 4.6	56.3 16.5	0.6
Bulges with both 5' and 3' G/U							
GCG U U	3.1	23.8	1.0	UAU G G	2.6	18.4	0.4
GUG U U	3.4	24.6	0.0	UGU G G	1.9 3.1	17.5 30.2	0.0

^aTop strand is written 5' → 3'.

^bValues calculated as described in text.

^cTotal number of single nucleotide group I bulge sequences with adjacent GU base pairs is 810.

^d(16)

Table 6
Group I Single Nucleotide Bulge Loop Thermodynamic Parameters

free energy increment for the insertion of a group I single nucleotide bulge loop into an RNA duplex	
$\Delta G^{\circ}_{37(\text{bulge loop})} = (-0.62 * \Delta G^{\circ}_{37(\text{less stable stem})}) + 0.25$ in kcal/mol	
nearest-neighbor bonus and penalty values	
$\begin{pmatrix} 5' & U & B & X \\ 3' & G & B & X \end{pmatrix}, \begin{pmatrix} 5' & G & B & G \\ 3' & G & B & X \end{pmatrix}, \text{ and } \begin{pmatrix} 5' & U & B & U \\ 3' & G & G & G \end{pmatrix}$	-0.6 kcal/mol
$\begin{pmatrix} 5' & G & B & X \\ 3' & U & Y & Y \end{pmatrix} \text{ and } \begin{pmatrix} 5' & U & X & B & U \\ 3' & Y & G & G & G \end{pmatrix}$	+0.4 kcal/mol
enthalpic increment for the insertion of a group I single nucleotide bulge loop into an RNA duplex	
$\Delta H^{\circ}_{(\text{bulge loop})} = +16.5$ in kcal/mol (independent of stem or nearest-neighbor effects)	